Patterning of Semiconductor Nanoparticles via Microcontact Printing

Xiao Chun Wu,[a] Li Feng Chi,*[a] and Harald Fuchs[a]

Keywords: Microcontact printing / Interaction / Interfaces / Nanocluster / Patterning / Semiconductors

Three general paths for patterning semiconductor nanoparticles stabilized with a short chain stabilizer via microcontact printing (μCP) are presented. The interface between the nanoparticles and surfaces has to be carefully designed to realize a successful direct or indirect printing.

Introduction

Parallel patterning of functional materials is very important for many photonic and electronic applications, for example multiple color LEDs, color pixels for field-emission displays, and multichannel chemical sensors. Therefore, the parallel schemes of positioning of these functional materials in predetermined areas are of great scientific and technological interest. Apart from the standard patterning techniques such as lithography, recently developed nontraditional patterning methods such as microcontact printing (μCP),[1] nanoimprinting lithography (NIL),[2] scanning probe lithography,[3] and dip-pen nanolithography[4] have attracted a great deal of attention in the field of surface patterning. Among them, μCP and NIL have the advantages of low-cost, simplicity, rapidity, and high throughput (parallel process). μCP is more versatile because many different materials can be used as inks to directly print on flat and curved surfaces.

Generally speaking, the patterning of functional materials can be realized in the following two ways. The first is where the distribution of the functional materials themselves on the surfaces is in a patterned way. Thus, the functionality is naturally patterned.[5–7] For example, Won et al. bound dendrimers on a surface, then let gold ions adsorb to the dendrimers. By UV irradiation with a photomask, patterned Au nanoparticle structures were obtained.[7] The other method is where functional materials are homogeneously distributed on surfaces while another material on top or beneath the functional material is patterned. In this way, through the inhibition or activation of the functionality of functional materials by printed materials, the functionality is realized in a patterned way.[8] For example, Wang et al. first assembled semiconductor nanoparticles on surfaces using a layer-by-layer strategy. Then copper grids were placed on top of the nanoparticle films as an optical mask. Because of the strong enhancement of photoluminescence (PL) from the nanoparticles by irradiation, a strong contrast in PL was observed after removal of the grids.[8]

By means of μCP, there are three possible paths to the patterning of the functional materials: (1) They can be selectively adsorbed to a printed heterogeneous surface, as shown in part a of Scheme 1. (2) They can be bound to a structured stamp and be directly printed on a homogeneous surface, as shown in part b of Scheme 1. (3) They can be brought to a homogeneous layer (e.g. spin coating) on a surface and be patterned by an inactive structure, as shown in Scheme 1 (see part c, the inactive structure can also be beneath the active layers). Although the direct printing of functional materials is desirable, it is not easy to achieve since a compatible stamp-molecule-surface system is needed. Successful printing requires detailed studies of various printing conditions such as ink concentration and time, printing time, and the surface properties of both the stamp and substrate. Therefore, compared to the printing of well-known systems for example self-assembled monolayers (SAMs), the direct printing of functional materials is more complicated.[9–12] Therefore, up to now, the realization of the patterning of functional materials via μCP has been mainly based on the direct printing of SAM layers, rather than the functional materials themselves.[13–17] The advantages of printing SAM layers are that they are relatively simple and the interaction mechanisms among ink, substrate, and stamp are well-studied in these systems,[18–20] but one more step for selective adsorption is needed. Should the first two methods prove difficult to realize, the third method may prove a good choice. For example, Koide et al. first printed alkyltrichlorosilane on an ITO glass substrate, then an organic light-emitting diode was deposited on the patterned substrate by a standard deposition technique.[14] Since the stamped SAM can impede the hole injection into

[a] Physikalisches Institut, Westfälische Wilhelms-Universität Münster and Center for Nanotechnology (CeNTech), 48149 Münster, Germany
E-mail: chi@uni-muenster.de

Supporting information for this article is available on the WWW under http://www.eurjic.org or from the author.

the hole transport layers, this renders the stamped area essentially nonemissive. Although the whole substrate was covered with LED materials, only unpatterned regions show effective emission. In this way, patterned LEDs were obtained.

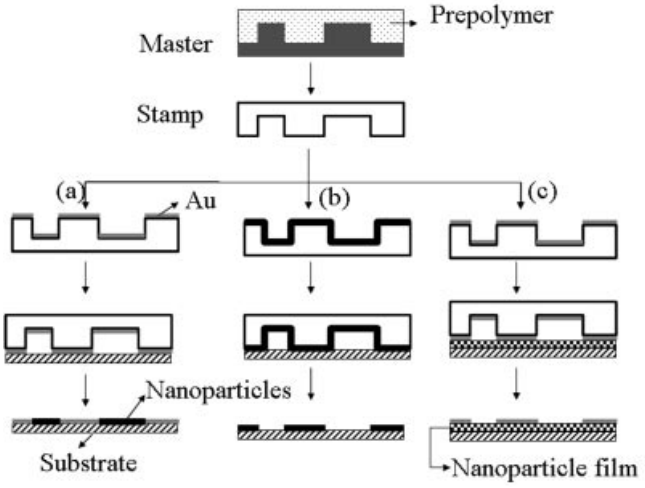

Scheme 1. Patterning of nanoparticles via (a) printing of block layer and adsorption of nanoparticles, (b) direct printing of nanoparticles, and (c) printing of block layer on the top of the nanoparticle layer.

Semiconductor nanoparticles show unique size-dependent optical properties and are of great interest for applications in optoelectronics, photovoltaics, and biological sensing.[21–25] Various chemical synthetic methods have been developed to prepare such nanoparticles. With the progress in the synthesis of nanoparticles using wet chemical syntheses, the synthesis of nanoparticles capped with so-called "stabilizers", which cap the surface of the nanoparticles during their growth, has been greatly improved and produced high-quality nanoparticles. Two different approaches have been developed to synthesize high-quality semiconductor nanoparticles. One is an organometallic synthesis based on the high-temperature thermolysis of precursors, first reported by Murray et al. in 1993,[26] and further improved later.[27–29] An alternative synthesis employs polyphosphates[30] or thiols[31,32] in aqueous media. With the success in obtaining high-quality nanoparticles, assembling them into devices becomes possible. Here we will explore the possibilities provided by the above-mentioned three paths to pattern high-quality CdTe nanoparticles stabilized with a short chain stabilizer (thioglycolic acid, TGA).

Results and Discussion

Selective Adsorption of Nanoparticles on a Patterned Surface

As mentioned in the introduction and shown in Scheme 1a, when nanoparticles show highly selective adsorption or binding onto certain surfaces, the patterning of them can be achieved through producing such surfaces in a patterned way. Recently, Loo et al. reported the direct printing of Au on a –SH terminated surface.[33] Here, we used this procedure to print a Au pattern and used this pattern as marks. Unprinted regions were further modified with different chemical groups in order to study the adsorption behaviors of a CdTe/TGA aqueous solution via hydrogen bonding, ligand exchange, or weak electrostatic forces. Part a of Figure 1 shows a topographic image of a printed Au line on a (3-mercaptoproply)trimethoxysilane (MPTMS) modified Si surface after the removal of MPTMS (O_2 plasma oxidation). A zoom-in image (not shown here) indicated that the unprinted region terminated with –OH groups was quite clean. After 3 h adsorption of a 1 mM CdTe/TGA aqueous solution, images were taken as shown in Figure 1 (b). CdTe nanoparticles showed random and inhomogeneous adsorption both on the hydrophilic –SiOH/Si surface and on the rough Au surface. The density of the nanoparticles was, however, very low. In the case of further modification with MPTMS, the thickness of the Au region increased to over 10 nm, indicating the formation of multilayers of MPTMS on the Au region. After adsorption of nanoparticles for 3 h, in the –SH region, we did not observe obvious adsorption (Supporting Information), indicating that no apparent ligand exchange was taking place between TGA and MPTMS. For (3-aminopropyl)dimethylethoxysilane (APDES) SAMs, the adsorption of nanoparticles on the $–NH_2$ region increased a lot compared to the case of the –SH terminated surface and showed less agglomeration than the –SiOH terminated surface, indicating greater electrostatic forces. However, the density of nanoparticles was still too low. Therefore, Scheme 1 (a) is not an effective path for patterning CdTe/TGA nanoparticles via simple hydrogen bonds, ligand exchange, and weak electrostatic forces.

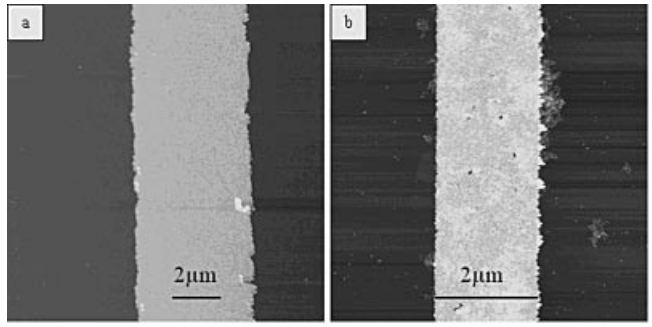

Figure 1. AFM images of Au patterns with –OH groups on unprinted regions before (a) and after (b) adsorption of a CdTe/TGA aqueous solution for 3 h.

Since the surface of the CdTe nanoparticle is capped with a layer of $SHCH_2COOH$ (TGA), the CdTe/TGA can in principle form multiple hydrogen bonds with the SiOH terminated surface. But the low-density inhomogeneous adsorption indicated that the hydrogen bonds between the TGA layer and the surface were weak and ineffective. This provides a hint that the TGA layer cannot be compared to some macromolecules for example poly(amidoamine) dendrimers. Dendrimer-stabilized nanoparticles show effective

adsorption on surfaces by multiple hydrogen bonds.[34] Here, the roughness of the surface might play a more important role as we could see that more particle aggregates adsorbed on the edges of the Au pattern and on the rough Au pattern. The formation of larger aggregates suggested that the interaction between the nanoparticles was stronger than that between the nanoparticles and the surface. The random adsorption of nanoparticles was also shown by the XPS measurements as signals of Cd, Te, and S from the nanoparticles were obtained (Supporting Information). For the –SH terminated surface, we did not see the obvious ligand exchange between TGA and MPTMS. The main reason for this was that TGA is not a viable ligand. For dodecylamine-stabilized CdSe/CdS core/shell nanoparticles, they showed strong adsorption on an $–NH_2$ or a –SH terminated surface because of strong ligand exchange.[35] This was also verified here by using tri-*n*-octylphosphane (TOPO) stabilized CdSe/CdS nanoparticles as shown in Figure 2. Figure 2 (a) shows an AFM image of printed Au on a –SH terminated surface. Figure 2 (b) presents the AFM image of this surface after adsorption of CdSe/CdS/TOPO in phenyloctane for 3 h. We could see a lot of nanoparticles dispersed on the –SH terminated regions because of strong exchange between TOPO and MPTMS. For the APDES modified surface, the positive charges are determined by the protonation of primary amino groups. The pK_a of the amino groups in solution is 10.6, it is lower in monolayers on solid substrates.[36] The surface pK_a of this layer is 3.9 by force titration and 4.3 by conventional contact angle wetting titration.[37] For a CdTe/TGA aqueous solution, the negative charges are determined by the deprotonation of carboxylate acid groups on the surface of the nanoparticles. The surface pK_a of –COOH terminated surfaces is 5.2 by electrochemical titration and 5.6 by contact angle titration.[38] In our case, the pH of the CdTe/TGA aqueous solution is ca. 7. Therefore the $–NH_2$ groups from the surface are basically uncharged and the –COOH groups from TGA are partially charged. This explains the low density of adsorption.

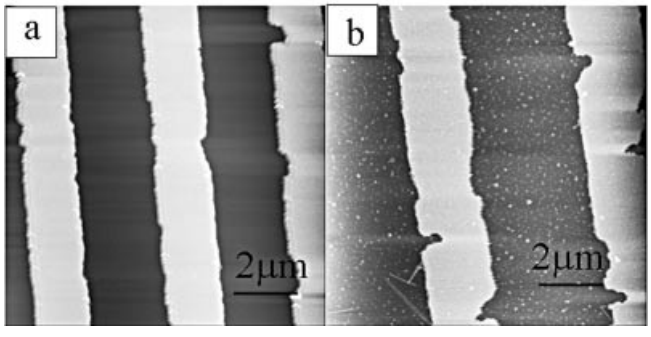

Figure 2. AFM images of Au patterns with –SH groups on unprinted regions before (a) and after (b) adsorption of a CdSe/TOPO solution for 3 h.

Direct Printing of Nanoparticles

We then followed Scheme 1 (b) to explore the possibility of directly printing nanoparticles. Although nanoparticles show no obvious adsorption on a hydrophilic OH terminated Si substrate, enough nanoparticles were left on the stamp by first adding 25 μL of nanoparticle dispersion to a hydrophilic stamp and then blowing it dry with N_2. Figures 3a, b, d, and e show topographic AFM images of printed nanoparticles at two different concentrations. At 1-mM concentration, nanoparticles can be printed homogeneously on the surface. The average height of nanoparticles is ca. 4.6 nm (Figure 3, c), similar to their diameter in solution. For the 2-mM concentration, the density of the nanoparticles on the printed regions was increased as expected. The average height of the nanoparticles is ca. 3.8 nm (Figure 3, e). This suggested that the nanoparticles mainly existed in the single form. Some larger aggregates of nanoparticles also formed at the 2-mM ink concentration as seen in Figure 3 (parts d and e), especially around the pattern edges. This has also been observed in the printing of other materials at higher ink concentrations.[39]

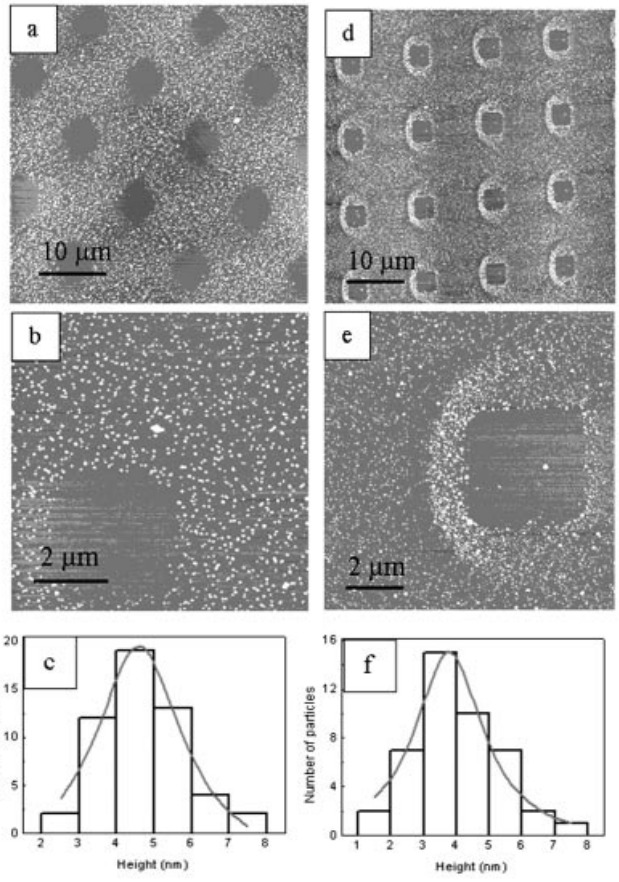

Figure 3. AFM images of printed CdTe/TGA nanoparticles on Si(100) surfaces with ink concentrations of 1 mM for (a) and (b) and of 2 mM for (d) and (e). Size distribution plots for (c) 1 mM and (f) 2 mM ink concentrations.

Printing Metal Structures on a Homogeneous Nanoparticle/Polymer Layer

For many practical applications, the stability of nanoparticles and the easiness of processing play very important

roles. It is therefore better to disperse the nanoparticles in a matrix, for example a polymer. Recently, Yang's group has succeeded in dispersing high-quality CdTe nanoparticles into polystyrene (PS) and polymethylmethacrylate (PMMA) blocks. The CdTe/PS block can be dissolved in chloroform and then easily spin-coated onto a Si (100) surface.[40] Wang et al. reported that metals deposited on stamps could be transferred to some polymer surfaces by printing above the glass transition temperatures of the polymers under certain pressures.[41] Here we found that metal transference could also be initiated at room temperature under pressure with a slightly longer printing time. Forty-nm Au was thermally evaporated on structured stamps. Through a conformal contact between the Au-coated stamp and the CdTe/PS/Si (100) substrate (1 h in contact with pressure), Au patterns were transferred to the substrate as shown in Figure 4 (a). The fluorescence of CdTe nanopaticles remained as evidenced by the optical bleaching of the fluorescence (Figure 4, b). The bright lines were derived from the gold scattering. The dark lines were from CdTe/PS films. Because of strong scattering from the gold, the photoluminescence from the nanoparticles was shadowed. Therefore, we used PL bleaching to verify the existence of the PL from the nanoparticles. The sample was first placed under a blue light for 10 min and then moved partially out of the irradiation region. A luminescence image was taken immediately after the movement. We could see that the part without the 10 min irradiation showed a strong PL in comparison with that with the 10 min irradiation. The gold part showed no bleaching. A pure CdTe/PS film on a Si substrate underwent a similar bleaching behavior as shown in Figure 4 (c).

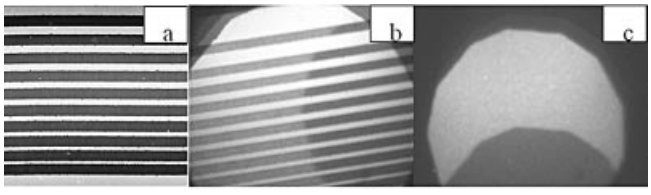

Figure 4. AFM (a) and luminescence (b) images of spin-coated CdTe/PS layer with printed Au patterns on top, and luminescence image (c) of spin-coated CdTe/PS layer.

In conclusion, we have presented several general strategies for the patterning of functional high-quality CdTe/TGA nanoparticles via μCP. Since the synthesis of CdTe/TGA nanoparticles is well-developed, a similar protocol can be adopted for the syntheses of other II-VI nanoparticles[31] or for the post-treatment of nanoparticle surfaces.[42] The patterning methods we have presented here therefore represent a general and easy process for the patterning of functional high-quality CdTe/TGA nanoparticles and also at the same time provide useful guides for patterning similar systems.

Experimental Section

A silicon substrate [WaferNet Co., Type N, 0.5 mm thick, orientation (100), resistivity 2–5 Ω cm] and SiO_2/Si substrate with 300-nm thick thermal SiO_2 were cut and ultrasonicated successively in acetone (p.a.), chloroform (p.a.), 2-propanol (p.a.), and water for 10 min. They were then cleaned with the standard RCA procedure: 15 min immersion into a 70 °C hot 1:1:5 mixture of NH_4OH (25%, Fluka, p.a.), H_2O_2 (31%, Fluka, p.a.) and water (Millipore, 18.2 MΩ cm); followed by a 15 min immersion into a 70 °C hot 1:1:5 mixture of HCl (37%, Aldrich, A.C.S. reagent), H_2O_2 (31%, Fluka, p.a) and water (Millipore, 18.2 MΩ cm). They were finally rinsed with water, and then dried under a stream of nitrogen. MPTMS (3-mercaptopropyltrimethoxysilane, 95%, Aldrich) and APDES [3-aminopropyl(dimethylethoxysilan), 97%, ABCR, Karlsruhe] SAMs were formed on SiO_2 surfaces by vapor deposition in a vacuum chamber for 15 h at room temperature. PDMS stamps (sylgard 184, Dow Corning) were formed on a patterned Si wafer master (IMS Stuttgart, before first use master was rendered hydrophobic with (fluoroalkyl)trichlorosilane vapor).

Printing of Au Structures: Au layers on hydrophobic stamps were deposited by thermal evaporation. A conformal contact between the Au-coated stamp and the MPTMS-modified (or PS-coated) Si substrate was initiated and kept for 1 min for the MPTMS-modified substrate and 1 h under pressure for the PS-coated substrate,[40] then the stamp was peeled off from the substrate. Because of the stronger interaction between Au and the substrate, Au patterns were transferred to the substrate. After 1 min 150-W O_2 plasma treatment, the SH region was oxidized and became an OH region (Templa System 100-E plasma system). This region can be used for further modification via silanization with different chemical groups.

Printing of Nanoparticles: A freshly activated stamp (1 mbar O_2 plasma, 300 W for 20 s) was covered with one drop (25 μL) of CdTe/TGA ink solution for 1 min, and then blown dry with N_2. It was put in a conformal contact with a clean Si (100) substrate for 25 s and then peeled off from the substrate.

Thioglycolic acid-capped CdTe (CdTe/TGA) nanocrystals (ca. 4 nm in size with a band edge photoluminescence maximum at 590 nm, 6% room-temperature quantum efficiency) in aqueous solution were obtained from the Photonics and Optoelectronics Group, Physics Department and CeNS, Ludwig-Maximilians Universität (Munich, Germany). CdTe nanoparticles distributed in a polystyrene (PS) block were obtained from the Key Lab of Supramolecular Structure and Materials, College of Chemistry, Jilin University, Changchun, P. R. China.

AFM measurements were performed with a commercial instrument (Digital Instruments, Nanoscope IIIa, Dimension 3000, Santa Barbara, CA) operated in tapping mode, silicon cantilevers (Nanosensors) of spring constant 250–350 kHz were used. XPS measurements were carried out with a VG ESCALAB 250 imaging XPS spectrometer. The samples were irradiated with monochromatic Al-K_α X-rays (15 kV, 150 W, 500 μm spot size).

Supporting Information Available: AFM images of the Au patterned surface with –SH and $–NH_2$ groups on un-patterned regions before and after adsorption of CdTe/TGA, as well as the XPS spectrum of the Au surface terminated with –OH groups after adsorption of CdTe/TGA.

Acknowledgments

This work was supported by DFG (CH-141). CdTe/TGA nanocrystals were kindly provided by Dr. A. L. Rogach from the Photonics and Optoelectronics Group, Physics Department and CeNS, Ludwig-Maximilians Universität (Munich, Germany) and the CdTe

nanoparticles distributed in a polystyrene (PS) block were kindly provided by Prof. B. Yang from the Key Lab of Supramolecular Structure and Materials, College of Chemistry, Jilin University, Changchun, P. R. China.

[1] Y. N. Xia, G. M. Whitesides, *Angew. Chem. Int. Ed.* **1998**, *37*, 551–575.
[2] S. Y. Chou, P. R. Krauss, P. J. Renstrom, *Science* **1996**, *272*, 85–87.
[3] R. M. Nyffenegger, R. M. Penner, *Chem. Rev.* **1997**, *97*, 1195–1230.
[4] R. D. Piner, J. Zhu, F. Xu, S. H. Hong, C. A. Mirkin, *Science* **1999**, *283*, 661–663.
[5] V. Erokhin, V. Troitsky, S. Erokhina, G. Mascetti, C. Nicolini, *Langmuir* **2002**, *18*, 3185–3190.
[6] F. Hua, T. H. Cui, Y. Lvov, *Langmuir* **2002**, *18*, 6712–6715.
[7] J. Won, K. J. Ihn, Y. S. Kang, *Langmuir* **2002**, *18*, 8246–8249.
[8] Y. Wang, Z. Y. Tang, M. A. Correa-Duarte, L. M. Liz-Marzan, N. A. Kotov, *J. Am. Chem. Soc.* **2003**, *125*, 2830–2831.
[9] A. Bernard, J. P. Renault, B. Michel, H. R. Bosshard, E. Delamarche, *Adv. Mater.* **2000**, *12*, 1067–1070.
[10] J. Hyun, Y. J. Zhu, A. Liebmann-Vinson, T. P. Beebe, A. Chilkoti, *Langmuir* **2001**, *17*, 6358–6367.
[11] H. Kind, J. M. Bonard, C. Emmenegger, L. O. Nilsson, K. Hernadi, E. Maillard-Schaller, L. Schlapbach, L. Forro, K. Kern, *Adv. Mater.* **1999**, *11*, 1285–1289.
[12] H. Kind, M. Geissler, H. Schmid, B. Michel, K. Kern, E. Delamarche, *Langmuir* **2000**, *16*, 6367–6373.
[13] E. Delamarche, H. Schmid, A. Bietsch, N. B. Larsen, H. Rothuizen, B. Michel, H. Biebuyck, *J. Phys. Chem. B* **1998**, *102*, 3324–3334.
[14] K. Ha, Y. J. Lee, D. Y. Jung, J. H. Lee, K. B. Yoon, *Adv. Mater.* **2000**, *12*, 1614–1617.
[15] Y. Harada, X. L. Li, P. W. Bohn, R. G. Nuzzo, *J. Am. Chem. Soc.* **2001**, *123*, 8709–8717.
[16] Y. Koide, Q. W. Wang, J. Cui, D. D. Benson, T. J. Marks, *J. Am. Chem. Soc.* **2000**, *122*, 11266–11267.
[17] Y. N. Xia, G. M. Whitesides, *J. Am. Chem. Soc.* **1995**, *117*, 3274–3275.
[18] T. Franzl, D. S. Koktysh, T. A. Klar, A. L. Rogach, J. Feldmann, N. Gaponik, *Appl. Phys. Lett.* **2004**, *84*, 2904–2906.
[19] Y. L. Loo, R. L. Willett, K. W. Baldwin, J. A. Rogers, *J. Am. Chem. Soc.* **2002**, *124*, 7654–7655.
[20] Y. N. Xia, M. Mrksich, E. Kim, G. M. Whitesides, *J. Am. Chem. Soc.* **1995**, *117*, 9576–9577.
[21] A. P. Alivisatos, *Science* **1996**, *271*, 933–937.
[22] M. G. Bawendi, M. L. Steigerwald, L. E. Brus, *Annu. Rev. Phys. Chem.* **1990**, *41*, 477–496.
[23] N. Chestnoy, T. D. Harris, R. Hull, L. E. Brus, *J. Phys. Chem.* **1986**, *90*, 3393–3399.
[24] A. Henglein, *Top. Curr. Chem.* **1988**, *143*, 113–180.
[25] M. L. Steigerwald, L. E. Brus, *Acc. Chem. Res.* **1990**, *23*, 183–188.
[26] C. B. Murray, D. J. Norris, M. G. Bawendi, *J. Am. Chem. Soc.* **1993**, *115*, 8706–8715.
[27] X. G. Peng, M. C. Schlamp, A. V. Kadavanich, A. P. Alivisatos, *J. Am. Chem. Soc.* **1997**, *119*, 7019–7029.
[28] Z. A. Peng, X. G. Peng, *J. Am. Chem. Soc.* **2001**, *123*, 183–184.
[29] Z. A. Peng, X. G. Peng, *J. Am. Chem. Soc.* **2002**, *124*, 3343–3353.
[30] L. Spanhel, M. Haase, H. Weller, A. Henglein, *J. Am. Chem. Soc.* **1987**, *109*, 5649–5655.
[31] N. Gaponik, D. V. Talapin, A. L. Rogach, K. Hoppe, E. V. Shevchenko, A. Kornowski, A. Eychmuller, H. Weller, *J. Phys. Chem. B* **2002**, *106*, 7177–7185.
[32] A. Rogach, A. Susha, F. Caruso, G. Sukhorukov, A. Kornowski, S. Kershaw, H. Mohwald, A. Eychmuller, H. Weller, *Adv. Mater.* **2000**, *12*, 333–337.
[33] Y. L. Loo, R. L. Willett, K. W. Baldwin, J. A. Rogers, *Appl. Phys. Lett.* **2002**, *81*, 562–564.
[34] X. C. Wu, A. M. Bittner, K. Kern, *Adv. Mater.* **2004**, *16*, 413–417.
[35] T. Vossmeyer, S. Jia, E. Delonno, M. R. Diehl, S. H. Kim, X. Peng, A. P. Alivisatos, J. R. Heath, *J. Appl. Phys.* **1998**, *84*, 3664–3670.
[36] Z. Y. Tang, Y. Wang, N. A. Kotov, *Langmuir* **2002**, *18*, 7035–7040.
[37] D. V. Vezenov, A. Noy, L. F. Rozsnyai, C. M. Lieber, *J. Am. Chem. Soc.* **1997**, *119*, 2006–2015.
[38] J. W. Zhao, L. Q. Luo, X. R. Yang, E. K. Wang, S. J. Dong, *Electroanalysis* **1999**, *11*, 1108–1111.
[39] T. Pompe, A. Fery, S. Herminghaus, A. Kriele, H. Lorenz, J. P. Kotthaus, *Langmuir* **1999**, *15*, 2398–2401.
[40] H. Zhang, Z. C. Cui, Y. Wang, K. Zhang, X. L. Ji, C. L. Lu, B. Yang, M. Y. Gao, *Adv. Mater.* **2003**, *15*, 777–780.
[41] Z. Wang, J. F. Yuan, J. Zhang, R. B. Xing, D. H. Yan, Y. C. Han, *Adv. Mater.* **2003**, *15*, 1009–1012.
[42] Y. Babayan, J. E. Barton, E. C. Greyson, T. W. Odom, *Adv. Mater.* **2004**, *16*, 1341–1345.

Received: June 10, 2005
Published Online: August 29, 2005

